Methods to study the mitochondrial unfolded protein response (UPR^{mt}) in *Caenorhabditis elegans*

Simon Haeussler[1] and Barbara Conradt[2]

Author Affiliations

1 Faculty of Biology, Ludwig-Maximilians-University Munich, 82152 Planegg-Martinsried, Germany

2 Research Department of Cell and Developmental Biology, Division of Biosciences, University College London, London WC1E 6AP, United Kingdom; Email: b.conradt@ucl.ac.uk

Running Head

Methods in *C. elegans* UPR^{mt} research (36/60 characters)

Abstract

The nematode *Caenorhabditis elegans* is a powerful model to study cellular stress responses. Due to its transparency and ease of genetic manipulation, *C. elegans* is especially suitable for fluorescence microscopy. As a result, studies of *C. elegans* using different fluorescent reporters have led to the discovery of key players of cellular stress response pathways, including the mitochondrial unfolded protein response (UPR^{mt}). UPR^{mt} is a protective retrograde signaling pathway that ensures mitochondrial homeostasis. The nuclear genes *hsp-6* and *hsp-60* encode mitochondrial chaperones and are highly expressed upon UPR^{mt} induction. The transcriptional reporters of these genes, *hsp-6::gfp* and *hsp-60::gfp*, have been instrumental for monitoring this pathway in live animals. Additional tools for studying UPR^{mt} include fusion proteins of ATFS-1 and DVE-1, ATFS-1::GFP and DVE-1::GFP, key players of the UPR^{mt} pathway. In this protocol, we discuss advantages and limitations of currently available methods and reporters, and we provide detailed instructions on how to image and quantify reporter expression.

Key words

UPR^{mt} reporters, *hsp-6*, *hsp-60*, *dve-1*, *atfs-1*, *gfp*

1. Introduction

The nematode *Caenorhabditis elegans* has been used as a model in cell and developmental biology for more than 50 years ***(1,2)***. Its cost-effective maintenance, short life cycle, transparency and ease of genetic manipulation by forward and reverse genetics makes *C. elegans* an excellent model system ***(3)***. In addition, many metabolic pathways and genes associated with human diseases are well conserved in *C. elegans* ***(4,5)*** and, hence, can be studied under physiological conditions both at the cellular and organismal level. Therefore, *C. elegans* is frequently used for studies in the fields of cellular stress responses and aging, among many others.

The mitochondrial unfolded protein response (UPR^{mt}) is a retrograde signaling pathway that is induced upon mitochondrial stress. It has been discovered in mammals ***(6,7)*** and studied extensively in *C. elegans*. Central players of this pathway were discovered in *C. elegans* through RNA-mediated interference (RNAi) screens using transcriptional reporters ***(8-13)***, and follow-up studies led to a broader understanding of UPR^{mt} and its regulation. Initially, it was described as an 'unfolded protein response' that acts to restore homeostasis in the mitochondrial matrix mainly through the transcriptional upregulation of cytoprotective genes encoding, for example, mitochondrial chaperones (e.g. HSP-6 and HSP-60) and proteases, as well as detoxifying enzymes ***(13)***. However, it has become evident that metabolic adaptation is also central to the response ***(10,14-19)***. The bZIP transcription factor 'activating transcription factor associated with stress 1' (ATFS-1) is the master regulator of UPR^{mt} and, together with the transcription factor DVE-1, induces a broad transcriptional program upon mitochondrial stress ***(9,11,19,20)***.

The UPR^{mt} pathway can be monitored using different approaches. The induction or suppression of transcriptional *gfp* reporters of the chaperone genes *hsp-6* and *hsp-60* can be measured, both

in a qualitative and quantitative manner. Moreover, translocation of fluorescent fusion proteins of ATFS-1::GFP ***(21)*** or DVE-1::GFP ***(9)*** can be recorded and used as a read-out. Furthermore, transcript levels of known UPR^{mt} effectors (e.g. *hsp-6*, *hsp-60* or *timm-23*) can be determined by quantitative reverse transcription polymerase chain reaction (RT-qPCR), or protein levels of the aforementioned UPR^{mt} effectors can be determined and quantified by western blot analysis.

Antibodies against endogenous ATFS-1 ***(20)*** and HSP-6 proteins ***(22)*** have been developed but are available only upon request, while an antibody against *C. elegans* HSP-60 ***(23)*** is commercially available at 'Developmental Studies Hybridoma Bank (DSHB)' (https://dshb.biology.uiowa.edu/HSP60). However, depending on the strain of interest, the collection of sufficient amounts of staged worms for western blot analysis may be tedious and time consuming. In addition, UPR^{mt} has been described as a transcriptional response, and discrepancies have been reported between changes observed at the transcriptional level and the level of endogenous protein ***(14)***.

Measuring mRNA levels upon induction of UPR^{mt} by RT-qPCR has also been used in the field to monitor UPR^{mt} ***(9,10,16,20,21,24-26)***. However, establishing RT-qPCR standards and protocols may require some effort, unless they are not already established in your laboratory. In addition, concerns have been raised about the reproducibility of published RT-qPCR results ***(27,28)***, even though it is one of the most commonly used molecular techniques to date.

For these reasons, the use of *gfp* reporters has proven to be a highly efficient method to monitor UPR^{mt}, and we will describe the use of the two fusion proteins ATFS-1::GFP and DVE-1::GFP, as well as transcriptional *gfp* reporters of *hsp-6* (*zcIs13*, *bcSi9*) and *hsp-60* (*zcIs9*) in more detail in this protocol.

2. Materials

2.1 Available reporter strains

1. P*atfs-1*::*atfs-1*::*gfp* (no allele or strain name available in ***(21)***)

2. SJ4197 P*dve-1*::*dve-1*::*gfp (zcIs39)*

3. SJ4100 P*hsp-6*::*gfp*::*unc-54 3'UTR (zcIs13)*

4. SJ4058 P*hsp-60*::*gfp*::*unc-54 3'UTR (zcIs9)*

5. MD3699 P*hsp-6*::*gfp*::*unc-54 3'UTR (bcSi9)*

2.2 Buffers and solutions

1. M9 buffer (5.8 g Na_2HPO_4, 3 g KH_2PO_4, 0.5 g NaCl, 1g NH_4Cl, H_2O to 1 liter. Sterilize by autoclaving)

2. Agarose pads (2% Agarose in ddH_20)

3. Anesthetic solutions: Sodium azide solution (10 mM in M9 buffer) or Levamisol solution (0.1 mM in M9 buffer)

2.3 Microscope

1. Fluorescence stereo microscope with camera and computer attached (e.g. Leica M205 FA)

3. Methods

3.1 Considerations for selecting the appropriate transgene

In *C. elegans*, *gfp* transgenes can be introduced as multi-copy extra-chromosomal arrays, which are transmitted to a certain fraction of the progeny and which can be integrated randomly into the genome ***(29)***. Alternatively, single copies of *gfp* transgenes can be integrated at defined chromosomal locations using either MosSCI ***(30,31)*** or CRISPR/CAS9 ***(32)***. In general, multi-copy transgenes are expressed at high levels due to their multi-copy nature and appear bright by fluorescence microscopy. However, some multi-copy transgenes affect brood size (e.g. *zcIs13*), especially in combination with RNAi or in certain genetic backgrounds. Single-copy integrated transgenes, on the other hand, tend to be less bright by fluorescence microscopy and may require the use of more sophisticated methodology for image acquisition and -analysis. Moreover, in *C. elegans*, both multi-copy and single-copy transgenes are often silenced in the germline and therefore can affect expression during embryogenesis. Thus, these transgenes cannot be used for studies during embryonic development.

3.1.1 The fusion proteins ATFS-1::GFP and DVE-1::GFP

The *atfs-1::gfp* transgene is expressed from the endogenous *atfs-1* promotor and consists of the genomic sequence of *atfs-1* fused at the 3'end of its coding region to *gfp*, which allows monitoring of the translocation of ATFS-1::GFP protein into the nucleus upon UPR^{mt} induction ***(21)***. Translocation of ATFS-1::GFP has so far only been observed in the two most proximal intestinal cells ***(20,21)***. Moreover, animals need to be challenged by severe mitochondrial stress in order to see ATFS-1::GFP translocation into the nucleus and even then, translocation can be

observed only in about 38% of the animals (Figure 1). For these reasons, this transgene is not commonly used in the field; nevertheless, it may be useful in very specific cases.

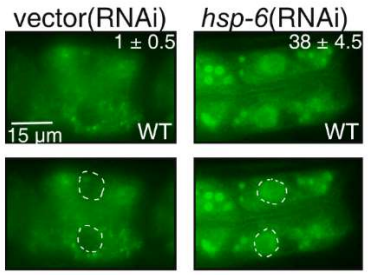

Figure 1: ATFS-1::GFP in intestinal cells of *C. elegans*. Fluorescence images of wild-type animals (L3 larvae) expressing an extra-chromosomal array of P_{atfs-1}*::atfs-1::gfp*, treated with empty *vector(RNAi)* or *hsp-6(RNAi)* (from ***(21)***). The most proximal intestinal cells are shown. The mean percentage of worms in which the ATFS-1::GFP fusion protein translocates into the nucleus upon RNAi-treatment is indicated in the upper right corner ± standard error of mean (SEM).

The *dve-1::gfp* transgene was constructed early on ***(9)*** and has been used in subsequent studies, either to measure UPR^{mt} induction or to specifically monitor DVE-1::GFP translocation into the nucleus upon mitochondrial stress ***(21,24,26,33,34)***. The integrated multi-copy array of *dve-1::gfp* was constructed from cDNA and is expressed from the endogenous *dve-1* promotor. Transgene expression is strongest in intestinal cells where translocation of DVE-1::GFP can be detected (Figure 2).

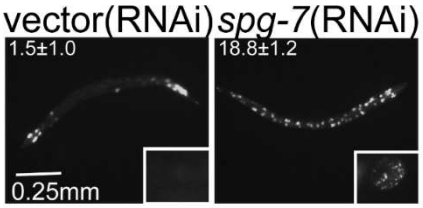

Figure 2: DVE-1::GFP in intestinal cells of *C. elegans*. Fluorescence images of wild-type animals (adults) expressing the integrated multi-copy transgene P_{dve-1}*::dve-1::gfp (zcIs39)*, treated with empty *vector(RNAi)* or *spg-7(RNAi)* (from ***(9)***). The number of intestinal cells per animal with DVE-1::GFP puncta in the nucleus is indicated in the upper right corner ± SEM. The inset in the lower right corner shows a high-magnification of an intestinal nucleus.

3.1.2 Transcriptional *gfp* reporters of *hsp-6* and *hsp-60*

The two most frequently used tools to monitor UPR^{mt} in the literature are multi-copy transcriptional reporters of *hsp-6* (transgene *zcIs13*) and *hsp-60* (transgene *zcIs9*), which were described in the first report of UPR^{mt} in *C. elegans* ***(13)***. Both transgenes are expressed under the control of the respective endogenous promoter (*hsp-6* and *hsp-60* promotors) and additionally contain the first 30 (*zcIs13*) or 21 (*zcIs9*) nucleotides of their 5' flanking region after the start codon, fused to *gfp*. Upon mitochondrial stress, both *zcIs13* and *zcIs9* are highly expressed in intestinal cells of all larval stages (L1-L4) and in adults. In some cases, expression can also be observed in body wall muscle cells, hypodermal cells and/or individual neurons but this can vary drastically between animals within a population. Moreover, the inter-individual variability of *zcIs13* expression within a population has been shown to be comparably high ***(14)*** and this can make it difficult to interpret results (e.g. in RNAi experiments).

In addition, strains carrying either transgene (*zcIs9*, *zcIs13*) have been shown to be hypersensitive in their responses to mitochondrial stress ***(13)***. Specifically, due to its strong induction upon mitochondrial stress (which makes it particularly useful for genome-wide RNAi screens), the *hsp-6* transgene *zcIs13* has been used more widely and is often favored over the *hsp-60* transgene *zcIs9* ***(8-12)***. However, the magnitude of induction of both transgenes should be interpreted with care due to their multicopy nature and low baseline expression under non-stressed conditions. Endogenous HSP-6 protein and its orthologs in other systems have been shown to be essential due to its housekeeping functions in mitochondrial protein import, as molecular chaperone and in quality control also under non-stressed conditions ***(35-41)***. Similarly, the chaperonin HSP-60 has important functions in mitochondrial protein folding and -homeostasis and, hence, is essential in eukaryotic cells ***(42,43)***. Consequently, both genes are highly expressed under non-stressed conditions ***(44-47)***, which is not reflected by the transgenes *zcIs9* and *zcIs13*.

An alternative therefore is the single-copy MosSCI integrated *hsp-6* transgene *bcSi9*, which is expressed more evenly among individuals of a population and shows a solid baseline expression ***(14)*** (Figure 3). The *bcSi9* transgene is essentially identical to the previously published *zcIs13* transgene, however, it is a single copy integration at a defined locus on chromosome IV. The expression of *bcSi9* in intestinal cells and muscle cells of the pharyngeal bulb is easily detectable by fluorescence microscopy using a stereo microscope, while expression in body wall muscle cells, hypodermal cells and neurons requires fluorescence microscopy with higher magnification (compound microscope). Because of its normal baseline expression under non-stressed conditions, the induction as well as suppression of the *bcSi9* transgene may appear rather subtle, as compared to other available transgenes. For this reason, it requires careful data acquisition and quantification, followed by statistical analysis.

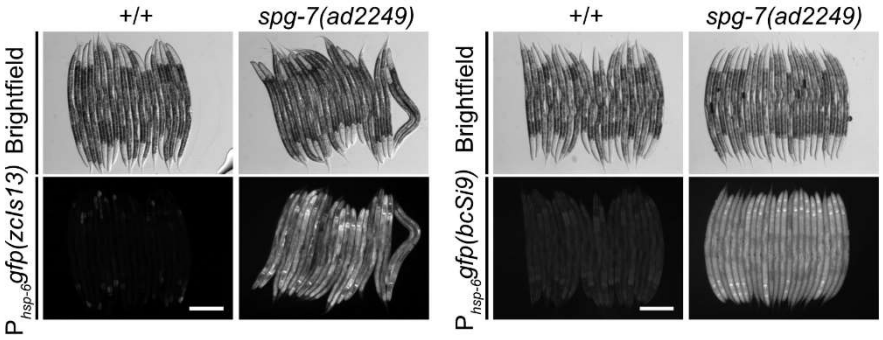

Figure 3: Expression of P*hsp-6::gfp (zcIs13)* and P*hsp-6::gfp (bcSi9)* transgenes in wild-type and *spg-7(ad2249)* animals. Fluorescence images of L4 larvae expressing the integrated multi-copy P*hsp-6::gfp (zcIs13)* and the single-copy P*hsp-6::gfp (bcSi9)* transgene, respectively (from ***(14)***). Both transgenes are predominantly expressed in the intestine of *C. elegans*. Scale bar: 200 µm.

In conclusion, there are a number of tools that can be used to monitor UPR^{mt} activation in live *C. elegans* animals. While the two fusion proteins ATFS-1::GFP and DVE-1::GFP may be advantageous in certain cases, the transcriptional *gfp* reporters of *hsp-6* and *hsp-60* can be used more widely. As previously discussed, the multi-copy transgenes *zcIs9* and *zcIs13* can preferably be used in high throughput analysis (e.g. RNAi screens). Moreover, results

generated with these transgenes may be further validated using other available methods that also include statistical analysis.

3.2 Preparation of microscope slides, image acquisition and -quantification

1. Prepare an agarose pad by dropping a 2% agarose solution onto a slide and place a second slide on top. Wait for the agarose solution to solidify (~1 minute) and carefully remove one of the slides. See note 1.

2. Pick ~20 staged worms from your plate of interest onto an unseeded NGM plate in order to free worms of any remaining bacteria. See notes 2, 3 and 4.

3. Add a drop (3 µl – 15 µl) of anesthetic solution onto the agarose pad. See notes 5 and 6.

4. Transfer ~20 worms into the drop of anesthetic solution and wait for its effect (~30 s). Once the worms do not move anymore, they can be arranged carefully with a pick or eye-lash tool. Try to arrange the worms as close to each other as possible. See note 7. Afterwards, carefully place a coverslip on top of the drop. See note 8.

5. Image worms using a fluorescence dissecting microscope with a filter for GFP excitation (excitation maximum at 488 nm). See notes 9, 10, 11 and 12.

6. Quantify fluorescence images using available tool sets for Fiji or comparable software and apply statistics to your results. See notes 13, 14 and 15.

4. Notes

1. It is useful to prepare a special ‘agar pad pouring area’. Simply glue two slides onto a surface with enough space to exactly fit another slide in between. The two glued slides will then serve as spacers to make sure the agarose pads are even.

2. Do not image worms of starved plates or plates that will starve soon. Reporter expression decreases drastically when starved worms are imaged. Maintain strains at least for two generations after starvation (or thawing) before imaging or starting any drug treatments or RNAi experiments.

3. Be careful to always pick worms of equal stage within one recording and across different experiments. Determine a useful stage in preliminary experiments. The effects of treatments may vary between stages and expression of the reporters varies drastically between the different stages. The L4 stage may be desirable for exact determination of developmental age (e.g. ‘Christmas tree vulva’). If adults are imaged, pick a decent amount of L4 larvae one day in advance to make sure you image adults of comparable age (e.g. day 1 adults).

4. When using RNAi or drug treatments that give a synthetic slow growth phenotype, make sure to image worms of these plates in a similar population density as controls. This may require the use of more worms when setting up the experiment and/or imaging on different days.

5. Sodium azide solution may be more preferable since worms tend to be more still and can be arranged nicely. Levamisol solution is a less potent anesthetic and worms tend to move a lot, even after a few minutes. Do not keep worms in anesthetic solution for longer than 10 min before imaging since worms tend to be stressed under these conditions. If you like to recover worms for other purposes after imaging, be aware that sodium azide inhibits the electron transport chain.

6. The volume of anesthetic solution needs to be adjusted. Beginners should start with a higher volume of anesthetic solution, as they might take more time to transfer the worms onto the agarose pad and arrange them.

7. For nice arrangement of worms, which makes representation and quantification at later stages much easier, break the surface tension of the drop using your pick or eye-lash tool. Repeat on all sides of the drop until a 'star-like puddle' forms. As soon as the liquid of the drop is distributed as described, worms in close proximity tend to collapse into their center and can be arranged easily.

8. Be quick but careful to add a coverslip on top. If too much time passes, the agar pad soaks up most of the anesthetic solution and air bubbles tend to get in between the worms when adding the coverslip, which may interfere with the fluorescent signal afterwards. More anesthetic solution can be added by pipetting at the sides of the coverslip if air bubbles occur.

9. Exposure time varies, depending on the reporter, experimental setup, magnification etc. and should be tested in preliminary runs. It may be required to test many different mutants or RNAi treatments in advance. Be aware that experimental temperature has an impact on *gfp* expression, both inside and outside of the incubator. Adjust exposure time in preliminary tests, using the samples with the highest and lowest expression level of the reporter (this can be different mutants, different RNAi's or different concentrations of drug treatments). Double-check not to overexpose your recordings.

10. The software of your microscope may support recordings with multiple exposure times at once, which may be desirable as well. Initial preliminary tests may not include all samples of a given study since sometimes, additional mutants or treatments may be tested at later stages. Having recorded previous experiments with many different exposure times at once may help

later, if an additional mutant expresses much higher or lower levels and the exposure time needs to be adjusted accordingly.

11. Always record at least two slides of each sample per run, including the controls. This will help in your statistical analysis later, after normalization to control values.

12. Additionally to fluorescence imaging, record a brightfield image each time, which can be used to generate a mask for subsequent quantification of fluorescence intensity using Fiji or other comparable software.

13. It may be sufficient to show a qualitative representation of your images but quantifying reporter expression allows for statistical analysis, which may be reassuring and may also be required at later steps.

14. Be aware that only images of equal exposure time and other settings like magnification, gain, etc. can be quantified within a dataset.

15. Different tool sets for fluorescence intensity measurements of images are available for Fiji and other comparable software. For segmentation and quantification of images of *hsp-6* (both *zcIs13* and *bcSi9)* and *hsp-60 (zcIs9)* reporters, a Fiji script is available in the supplemental information, Data S1 in ***(11)***. In brief, automated thresholding (e.g. Triangle method) is applied to either the fluorescence or brightfield image in order to generate a binary mask. Various auto-thresholding methods are available in Fiji, which can be tested. The Particle Analyzer of Fiji is applied in order to remove noise by setting a minimum size for objects to be included in the mask (~10 pixels). Subsequently, the mask is inverted and remaining unwanted objects can be removed manually. The mask is then applied to the corresponding fluorescence image in order to measure mean fluorescence intensity within a defined area of an image, preferably including all worms of an image. The mean fluorescence intensity outside the mask serves as background.

Acknowledgments

We thank Elisabeth Rackles and Stéphane G. Rolland for comments on the manuscript. This work was funded by the Deutsche Forschungsgemeinschaft (Co204/6-1 and CO204/9-1).

5. References

1. Brenner S (1974) The Genetics of *Caenorhabditis Elegans*. Genetics 1:71-94.

2. Sulston JE, Brenner S (1974) The DNA of *Caenorhabditis elegans*. Genetics 1:95-104.

3. Corsi AK, Wightman B, Chalfie M (2015) A Transparent Window into Biology: A Primer on *Caenorhabditis elegans*. Genetics 2:387-407.

4. Kim W, Underwood RS, Greenwald I, Shaye DD (2018) OrthoList 2: A New Comparative Genomic Analysis of Human and *Caenorhabditis elegans* Genes. Genetics 2:445-461.

5. Shaye DD, Greenwald I (2011) OrthoList: A Compendium of C. elegans Genes with Human Orthologs. PLoS One 5:e20085.

6. Martinus RD, Garth GP, Webster TL, Cartwright P, Naylor DJ, Høj PB, Hoogenraad NJ (1996) Selective Induction of Mitochondrial Chaperones in Response to Loss of the Mitochondrial Genome. Eur J Biochem 1:98-103.

7. Zhao Q, Wang J, Levichkin IV, Stasinopoulos S, Ryan MT, Hoogenraad NJ (2002) A mitochondrial specific stress response in mammalian cells. EMBO J 17:4411-4419.

8. Bennett CF, Vander Wende H, Simko M, Klum S, Barfield S, Choi H, Pineda VV, Kaeberlein M (2014) Activation of the mitochondrial unfolded protein response does not predict longevity in *Caenorhabditis elegans*. Nat Commun:3483.

9. Haynes CM, Petrova K, Benedetti C, Yang Y, Ron D (2007) ClpP mediates activation of a mitochondrial unfolded protein response in *C. elegans*. Dev Cell 4:467-480.

10. Liu Y, Samuel BS, Breen PC, Ruvkun G (2014) *Caenorhabditis elegans* pathways that surveil and defend mitochondria. Nature 7496:406-410.

11. Rolland SG, Schneid S, Schwarz M, Rackles E, Fischer C, Haeussler S, Regmi SG, Yeroslaviz A, Habermann B, Mokranjac D, Lambie E, Conradt B (2019) Compromised Mitochondrial Protein Import Acts as a Signal for UPR^{mt}. Cell Rep 7:1659-1669.e1655.

12. Runkel ED, Liu S, Baumeister R, Schulze E (2013) Surveillance-activated defenses block the ROS-induced mitochondrial unfolded protein response. PLoS Genet 3:e1003346.

13. Yoneda T, Benedetti C, Urano F, Clark SG, Harding HP, Ron D (2004) Compartment-specific perturbation of protein handling activates genes encoding mitochondrial chaperones. J Cell Sci Pt 18:4055-4066.

14. Haeussler S, Köhler F, Witting M, Premm MF, Rolland SG, Fischer C, Chauve L, Casanueva O, Conradt B (2020) Autophagy compensates for defects in mitochondrial dynamics. PLoS Genet 3:e1008638.

15. Kim S, Sieburth D (2018) Sphingosine Kinase Activates the Mitochondrial Unfolded Protein Response and Is Targeted to Mitochondria by Stress. Cell Rep 11:2932-2945.e2934.

16. Nargund Amrita M, Fiorese Christopher J, Pellegrino Mark W, Deng P, Haynes Cole M (2015) Mitochondrial and Nuclear Accumulation of the Transcription Factor ATFS-1 Promotes OXPHOS Recovery during the UPRmt. Mol Cell 1:123-133.

17. Oks O, Lewin S, Goncalves IL, Sapir A (2018) The UPR^{mt} Protects *Caenorhabditis elegans* from Mitochondrial Dysfunction by Upregulating Specific Enzymes of the Mevalonate Pathway. Genetics 2:457-473.

18. Ranji P, Rauthan M, Pitot C, Pilon M (2014) Loss of HMG-CoA Reductase in C. elegans Causes Defects in Protein Prenylation and Muscle Mitochondria. PLoS One 6:e100033.

19. Rauthan M, Ranji P, Aguilera Pradenas N, Pitot C, Pilon M (2013) The mitochondrial unfolded protein response activator ATFS-1 protects cells from inhibition of the mevalonate pathway. Proc Natl Acad Sci U S A 15:5981-5986.

20. Nargund AM, Pellegrino MW, Fiorese CJ, Baker BM, Haynes CM (2012) Mitochondrial Import Efficiency of ATFS-1 Regulates Mitochondrial UPR Activation. Science 6094:587-590.

21. Haynes CM, Yang Y, Blais SP, Neubert TA, Ron D (2010) The matrix peptide exporter HAF-1 signals a mitochondrial UPR by activating the transcription factor ZC376.7 in *C. elegans*. Mol Cell 4:529-540.

22. Köhler F, Müller-Rischart AK, Conradt B, Rolland SG (2015) The loss of *LRPPRC* function induces the mitochondrial unfolded protein response. Aging 9:701-712.

23. Hadwiger G, Dour S, Arur S, Fox P, Nonet ML (2010) A Monoclonal Antibody Toolkit for C. elegans. PLoS One 4:e10161.

24. Gao K, Li Y, Hu S, Liu Y (2019) SUMO peptidase ULP-4 regulates mitochondrial UPR-mediated innate immunity and lifespan extension. eLife:e41792.

25. Merkwirth C, Jovaisaite V, Durieux J, Matilainen O, Jordan Sabine D, Quiros Pedro M, Steffen Kristan K, Williams Evan G, Mouchiroud L, Tronnes Sarah U, Murillo V, Wolff Suzanne C, Shaw Reuben J, Auwerx J, Dillin A (2016) Two Conserved Histone Demethylases Regulate Mitochondrial Stress-Induced Longevity. Cell 5:1209-1223.

26. Tian Y, Garcia G, Bian Q, Steffen Kristan K, Joe L, Wolff S, Meyer Barbara J, Dillin A (2016) Mitochondrial Stress Induces Chromatin Reorganization to Promote Longevity and UPRmt. Cell 5:1197-1208.

27. Bustin S, Nolan T (2017) Talking the talk, but not walking the walk: RT-qPCR as a paradigm for the lack of reproducibility in molecular research. Eur J Clin Invest 10:756-774.

28. Taylor SC, Nadeau K, Abbasi M, Lachance C, Nguyen M, Fenrich J (2019) The Ultimate qPCR Experiment: Producing Publication Quality, Reproducible Data the First Time. Trends Biotechnol 7:761-774.

29. Mello CC, Kramer JM, Stinchcomb D, Ambros V (1991) Efficient gene transfer in C.elegans: extrachromosomal maintenance and integration of transforming sequences. EMBO J 12:3959-3970.

30. Frøkjær-Jensen C, Davis MW, Sarov M, Taylor J, Flibotte S, LaBella M, Pozniakovsky A, Moerman DG, Jorgensen EM (2014) Random and targeted transgene insertion in *Caenorhabditis elegans* using a modified Mos1 transposon. Nature Methods:529.

31. Frøkjær-Jensen C, Wayne Davis M, Hopkins CE, Newman BJ, Thummel JM, Olesen S-P, Grunnet M, Jorgensen EM (2008) Single-copy insertion of transgenes in *Caenorhabditis elegans*. Nature Genet:1375.

32. Chen C, Fenk LA, de Bono M (2013) Efficient genome editing in Caenorhabditis elegans by CRISPR-targeted homologous recombination. Nucleic Acids Res 20:e193-e193.

33. Berendzen KM, Durieux J, Shao L-W, Tian Y, Kim H-e, Wolff S, Liu Y, Dillin A (2016) Neuroendocrine Coordination of Mitochondrial Stress Signaling and Proteostasis. Cell 6:1553-1563.e1510.

34. Zhang Q, Wu X, Chen P, Liu L, Xin N, Tian Y, Dillin A (2018) The Mitochondrial Unfolded Protein Response Is Mediated Cell-Non-autonomously by Retromer-Dependent Wnt Signaling. Cell 4:870-883.e817.

35. Bhattacharyya T, Karnezis AN, Murphy SP, Hoang T, Freeman BC, Phillips B, Morimoto RI (1995) Cloning and Subcellular Localization of Human Mitochondrial hsp70. J Biol Chem 4:1705-1710.

36. Gambill BD, Voos W, Kang PJ, Miao B, Langer T, Craig EA, Pfanner N (1993) A dual role for mitochondrial heat shock protein 70 in membrane translocation of preproteins. J Cell Biol 1:109-117.

37. Kang P-J, Ostermann J, Shilling J, Neupert W, Craig EA, Pfanner N (1990) Requirement for hsp70 in the mitochondrial matrix for translocation and folding of precursor proteins. Nature 6297:137-143.

38. Kimura K, Tanaka N, Nakamura N, Takano S, Ohkuma S (2007) Knockdown of Mitochondrial Heat Shock Protein 70 Promotes Progeria-like Phenotypes in Caenorhabditis elegans. J Biol Chem 8:5910-5918.

39. Ran Q, Wadhwa R, Kawai R, Kaul SC, Sifers RN, Bick RJ, Smith JR, Pereira-Smith OM (2000) Extramitochondrial Localization of Mortalin/mthsp70/PBP74/GRP75. Biochem Biophys Res Commun 1:174-179.

40. Wadhwa R, Kaul SC, Mitsui Y, Sugimoto Y (1993) Differential Subcellular Distribution of Mortalin in Mortal and Immortal Mouse and Human Fibroblasts. Exp Cell Res 2:442-448.

41. Yokoyama K, Fukumoto K, Murakami T, Harada S-i, Hosono R, Wadhwa R, Mitsui Y, Ohkuma S (2002) Extended longevity of Caenorhabditis elegans by knocking in extra copies of hsp70F, a homolog of mot-2 (mortalin)/mthsp70/Grp75. FEBS Lett 1-3:53-57.

42. Bie AS, Cömert C, Körner R, Corydon TJ, Palmfeldt J, Hipp MS, Hartl FU, Bross P (2020) An inventory of interactors of the human HSP60/HSP10 chaperonin in the mitochondrial matrix space. Cell Stress Chaperones 3:407-416.

43. Cheng MY, Hartl FU, Martin J, Pollock RA, Kalousek F, Neuper W, Hallberg EM, Hallberg RL, Horwich AL (1989) Mitochondrial heat-shock protein hsp60 is essential for assembly of proteins imported into yeast mitochondria. Nature 6208:620-625.

44. Deocaris CC, Kaul SC, Wadhwa R (2008) From proliferative to neurological role of an hsp70 stress chaperone, mortalin. Biogerontology 6:391-403.

45. Kaul SC, Deocaris CC, Wadhwa R (2007) Three faces of mortalin: a housekeeper, guardian and killer. Exp Gerontol 4:263-274.

46. Radons J (2016) The human HSP70 family of chaperones: where do we stand? Cell Stress Chaperones 3:379-404.

47. Wadhwa R, Taira K, Kaul SC (2002) An Hsp70 family chaperone, mortalin/mthsp70/PBP74/Grp75: what, when, and where? Cell Stress Chaperones 3:309-316.